Aust. J. Phys., 1990, **43**, 373–87

Calculations on the Cosmic Ray Anisotropy above 10^{17} eV

A. G. K. Smith and R. W. Clay

Department of Physics and Mathematical Physics, University of Adelaide,
GPO Box 498, Adelaide, S.A. 5001, Australia.

Abstract

Possible trajectories of cosmic ray particles in our galactic magnetic field have been followed for various field models. It is found to be difficult to reconcile the observed low levels of cosmic ray anisotropy above 10^{18} eV with the modelled propagation. This strongly suggests a dominant extragalactic cosmic ray source at such high energies.

1. Introduction

The origin of cosmic rays with energies above 10^{17} eV is unknown. At lower energies evidence, from radio astronomy and gamma-ray astronomy in particular, suggests that known galactic objects can be associated with the origin of at least some of the energetic cosmic rays. These objects would include, for instance, supernova remnants and neutron star binary systems. At energies above 10^{17} eV, the situation is particularly unclear with some still controversial claims (e.g. Cassiday *et al.* 1989) for the observation of gamma rays from galactic sources but, on the whole with little evidence for any association with our galaxy. This is surprising from a naive point of view since, at the highest energies, charged cosmic rays should travel in almost straight lines in the galactic magnetic field and one would expect to see an effect of the non-isotropic galaxy around us (e.g. Clay 1987). Present measurements of the isotropy of observed cosmic rays show no clear evidence for any anisotropy above $\sim 10^{14}$ eV and the purpose of the present work is to see what limits might be set on models of the origin of ultra high energy galactic cosmic rays to be consistent with the measured upper limits.

2. Measurements of Cosmic Ray Anisotropy

Cosmic ray anisotropies may be measured by relatively simple apparatus since it is only the overall distribution of arrival directions on the sky which is of interest and angular resolution is not critical. The experimental difficulties are, however, demanding since careful allowance has to be made for any instrumental effects (mainly temperature dependent), the effect of varying atmospheric pressures, the effect of any instrument down-time and, ultimately, the effect of the motion of the earth through the cosmic ray gas (e.g. Murakami *et al.* 1990). At energies addressed in this paper, the measurements are limited

0004-9506/90/030373$03.00

by the low cosmic ray flux and it appears that measured upper limits simply reflect the numbers of events obtained in experiments (Clay 1987). Thus, it is random fluctuations in counts which dominate the results. Tradition has it that observational results are presented as first and second harmonics of the cosmic ray intensity distribution in Right Ascension at the observational latitude. This gives a very coarse view but, as will be indicated, should be suitable for testing galactic propagation models. Representative measured upper limits to the Right Ascension first harmonic anisotropy are 3% at 10^{17} eV, 10% at 10^{18} eV and 30% at 10^{19} eV (see e.g. Linsley and Watson 1977).

3. Anisotropy Simulations

Since cosmic rays are charged particles, their trajectories are determined by the structure of the galactic magnetic field between their source and the earth. In order to determine a predicted anisotropy, one has thus to make assumptions about the distribution of sources in the galaxy and also about the galactic magnetic field. Here, we assume that sources are uniformly distributed within the galactic plane and that one can then calculate a cosmic ray intensity for a given arrival direction at the earth by determining the path length travelled in the galaxy by a cosmic ray observed from that direction. In practice this is achieved by determining the galactic path length (proportional to the number of soruces intersected) of negatively charged particles (antiprotons) launched in particular directions from the earth. The basic galactic magnetic field model we use here is one proposed some time ago by Thielheim and Langhoff (1968) which reproduces many of the field properties deduced from astronomical (mainly pulsar) observations. More recent models (Lyne and Smith 1989; Rand and Kulkarni 1989) are available but this model has the advantage that it allows us to compare our results with previous such work and we will show that quite drastic modifications to the model make only limited changes to the conclusions.

The magnetic field model is basically one in which the field follows the direction of the spiral arms. It decreases with increasing distance from the galactic plane with a scale length of 175 pc and from the galactic centre (outside ~2 kpc) with a scale length of 10 kpc. The field reverses in direction at the galactic plane. The maximum field strength magnitude in the model is ~15 μG and at the earth it has a magnitude ~ 6 μG (1 $\mu\mathrm{G} \equiv 10^{-10}$ T). The values we use give a similar field structure to that considered by Berezinski and Mikhailov (1983, 1987) with about twice the field strength. Antiproton paths are found through the field model from the 'earth' using the Runge–Kutta method with a step length appropriate to the chosen antiproton energy, bearing in mind likely magnitudes of the magnetic field.

Sky distributions of path lengths were obtained typically by following ~25 000 paths for each map. This process becomes increasingly time consuming as lower energies are studied and becomes prohibitively long below ~3×10^{16} eV. Maps have been obtained by Karakula *et al.* (1971) and our maps are in good general agreement with theirs. However, their results were limited in the number of propagation parameters tested and the number of paths investigated for each map was low (146).

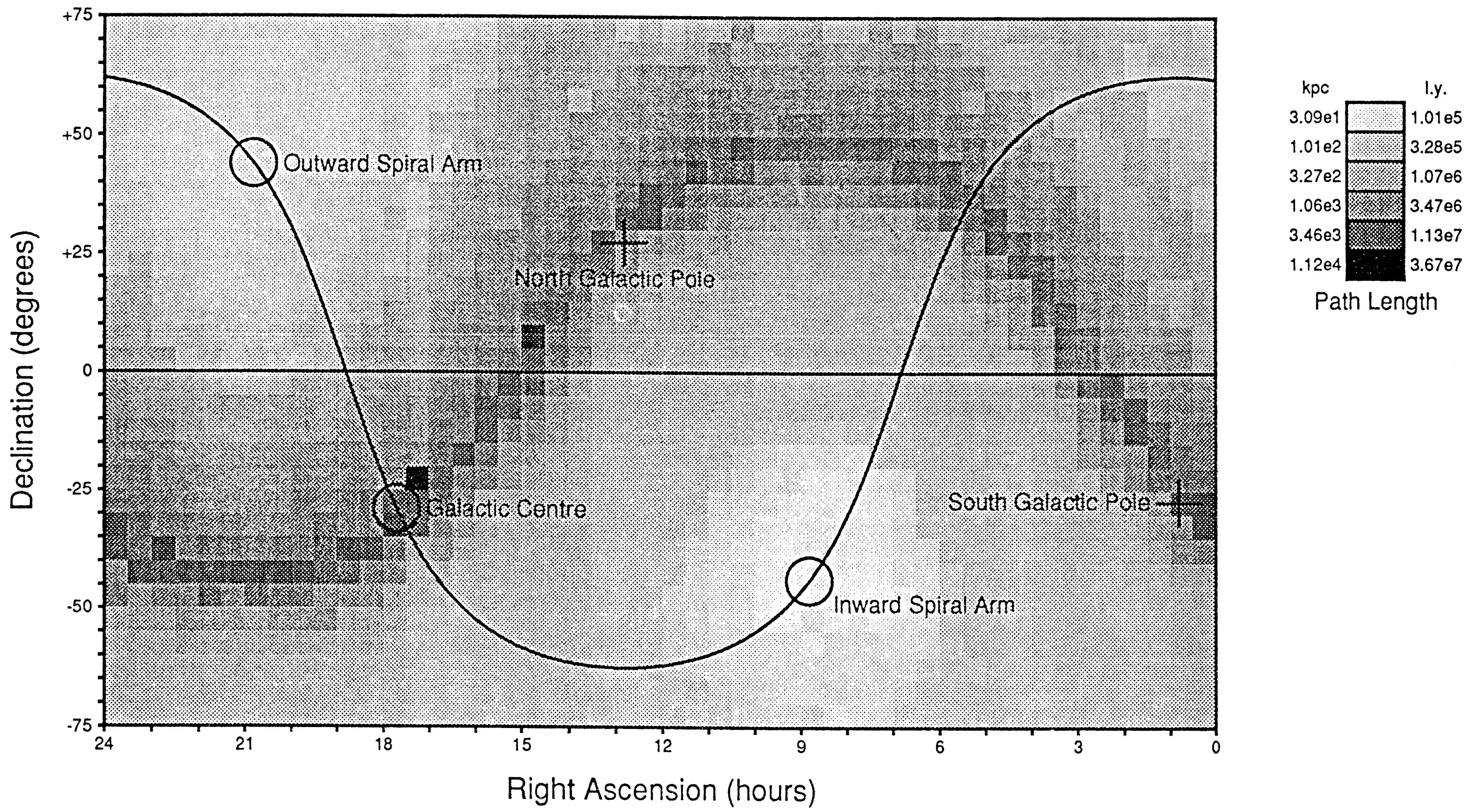

Fig. 1. Path length distributions within our galaxy for antiprotons fired from earth as a function of equatorial coordinates. A standard Thielheim–Langhoff model was assumed. (*a*) Antiprotons of energy 10^{17} eV (above). (*b*) Antiprotons of energy 10^{18} eV (p. 376). (*c*) Antiprotons of energy 10^{19} eV (p. 377).

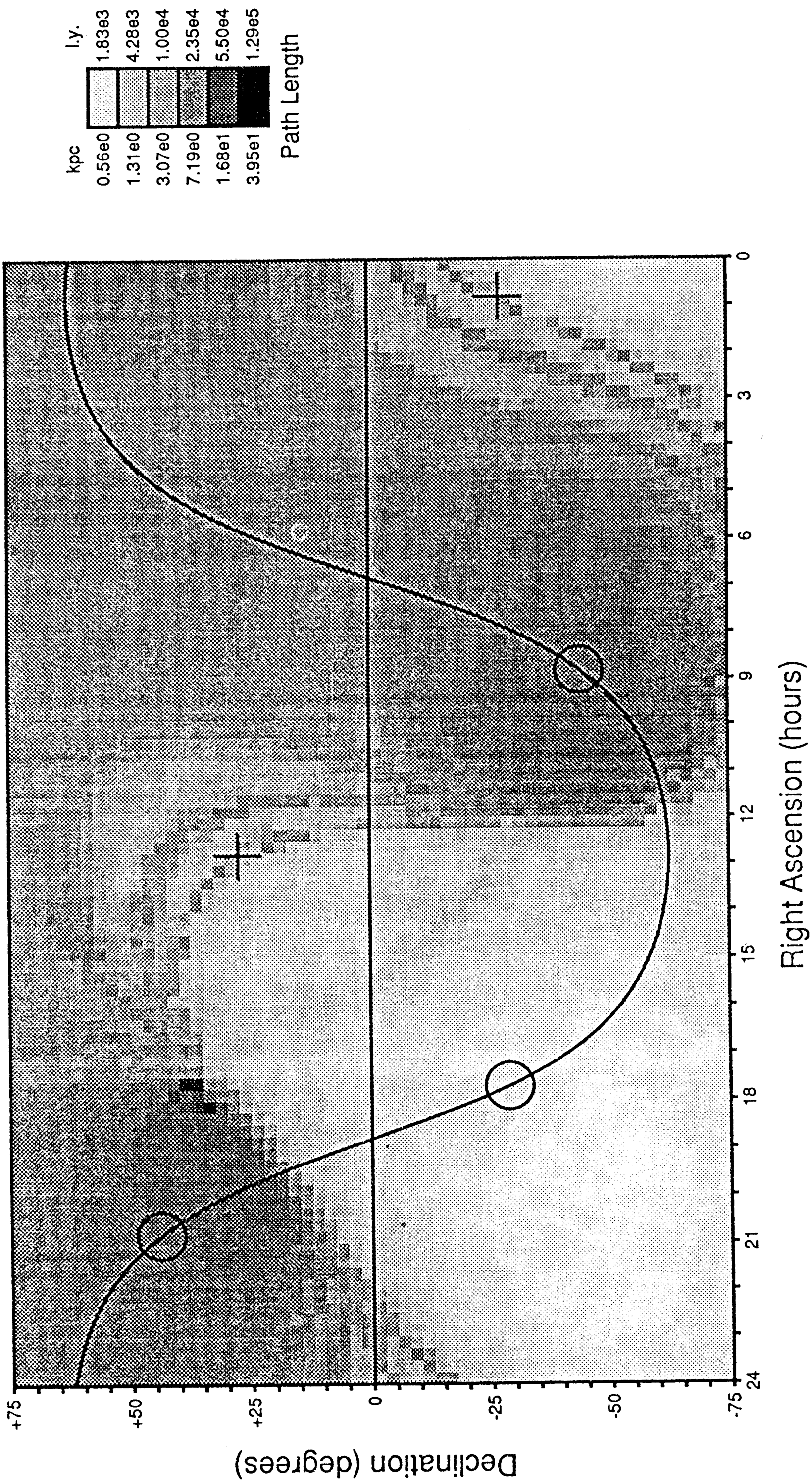
kpc
0.56e0
1.31e0
3.07e0
7.19e0
1.68e1
3.95e1
l.y.
1.83e3
4.28e3
1.00e4
2.35e4
5.50e4
1.29e5
Path Length
Declination (degrees)
+75
+50
+25
0
-25
-50
-75
Right Ascension (hours)
24
21
18
15
12
9
6
3
0

Fig. 1b

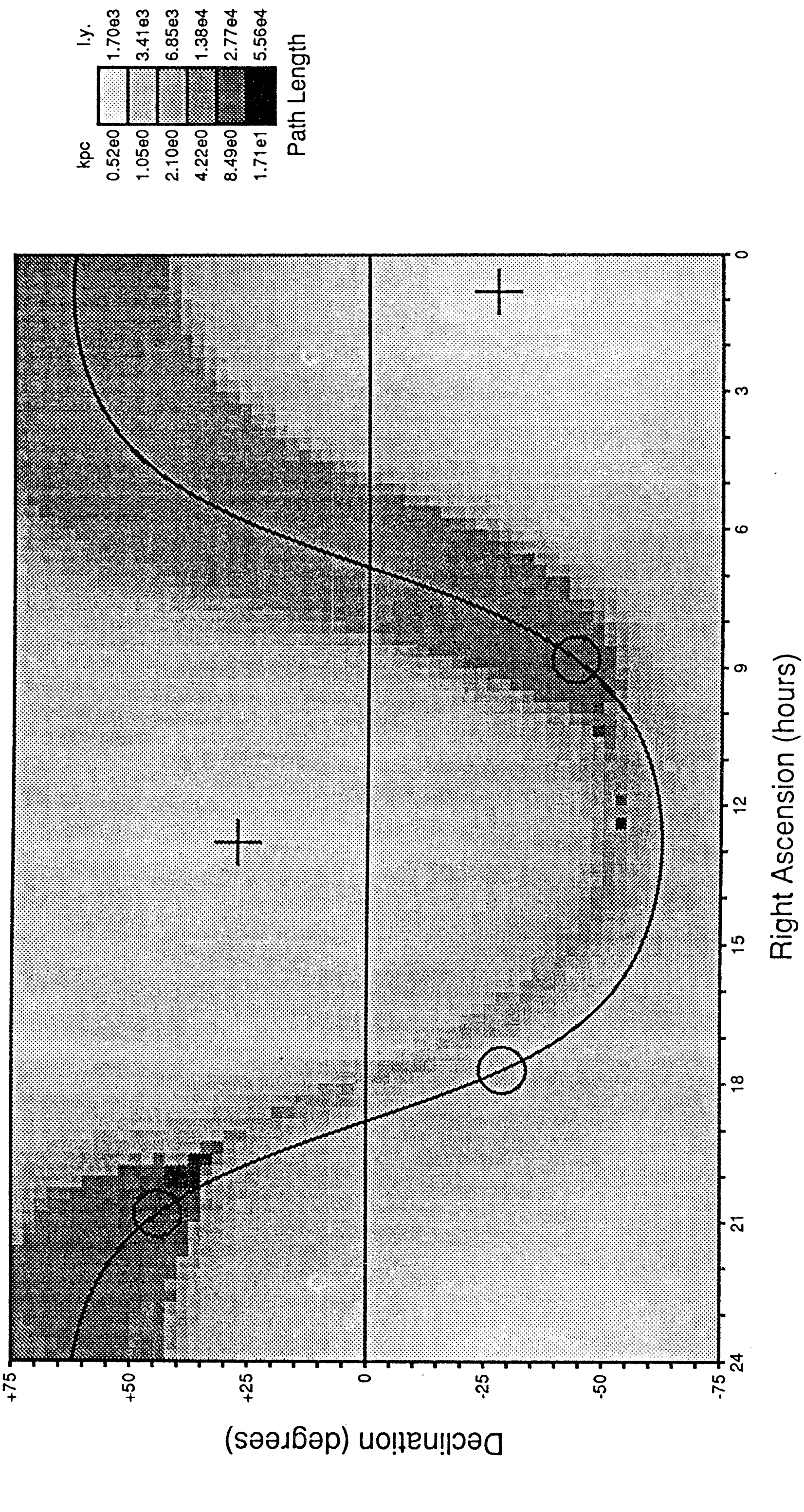
kpc
0.52e0
1.05e0
2.10e0
4.22e0
8.49e0
1.71e1
l.y.
1.70e3
3.41e3
6.85e3
1.38e4
2.77e4
5.56e4
Path Length
Declination (degrees)
+75
+50
+25
0
-25
-50
-75
Right Ascension (hours)
24
21
18
15
12
9
6
3
0

Fig. 1c

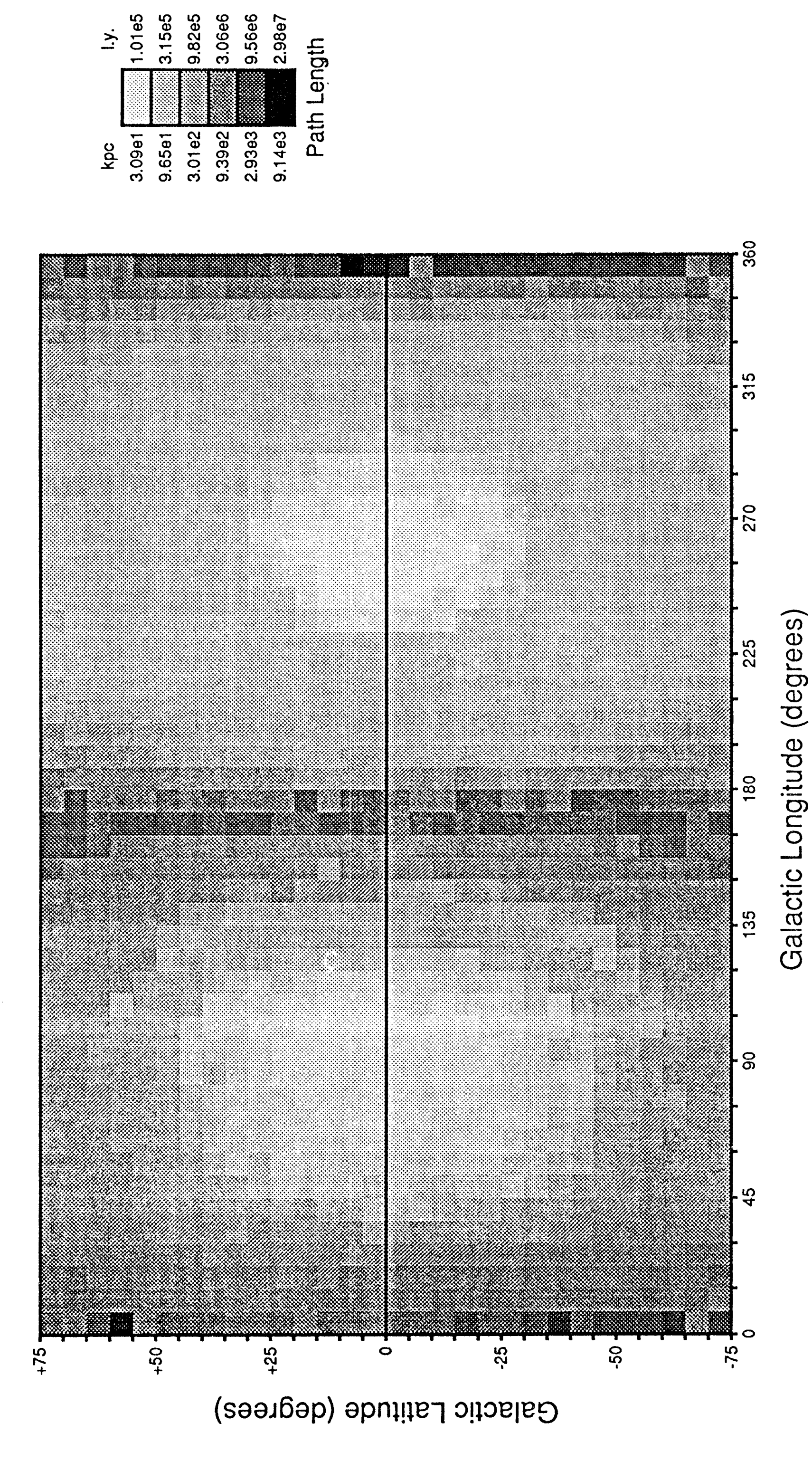

Fig. 2. Path length distributions as for Fig. 1 but using galactic coordinates: *(a)* 10^{17} eV (above); *(b)* 10^{18} eV (p. 379); *(c)* 10^{19} eV (p. 380).

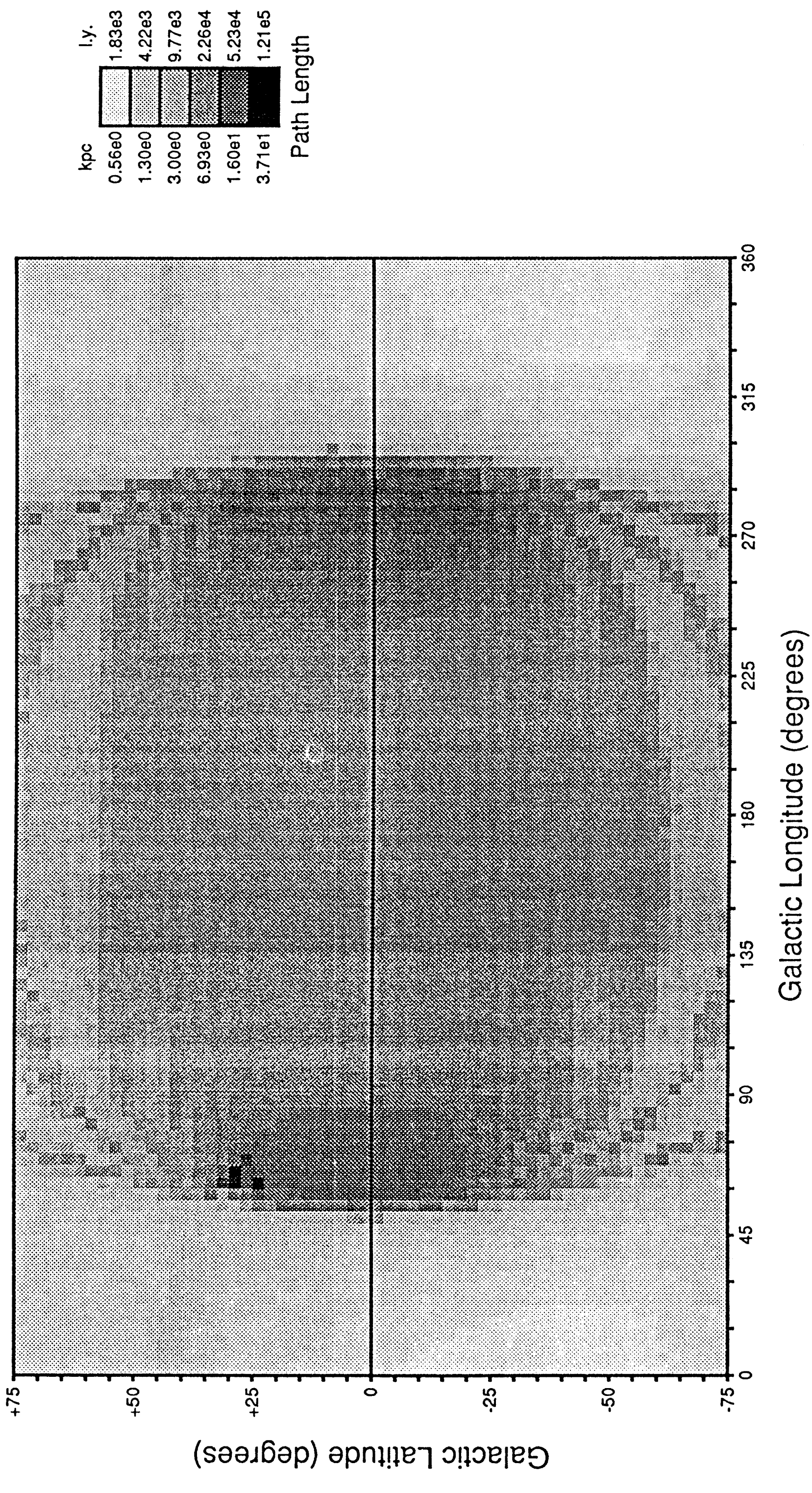
kpc
0.56e0
1.30e0
3.00e0
6.93e0
1.60e1
3.71e1
l.y.
1.83e3
4.22e3
9.77e3
2.26e4
5.23e4
1.21e5
Path Length
Galactic Latitude (degrees)
+75
+50
+25
0
-25
-50
-75
Galactic Longitude (degrees)
0
45
90
135
180
225
270
315
360

Fig. 2b

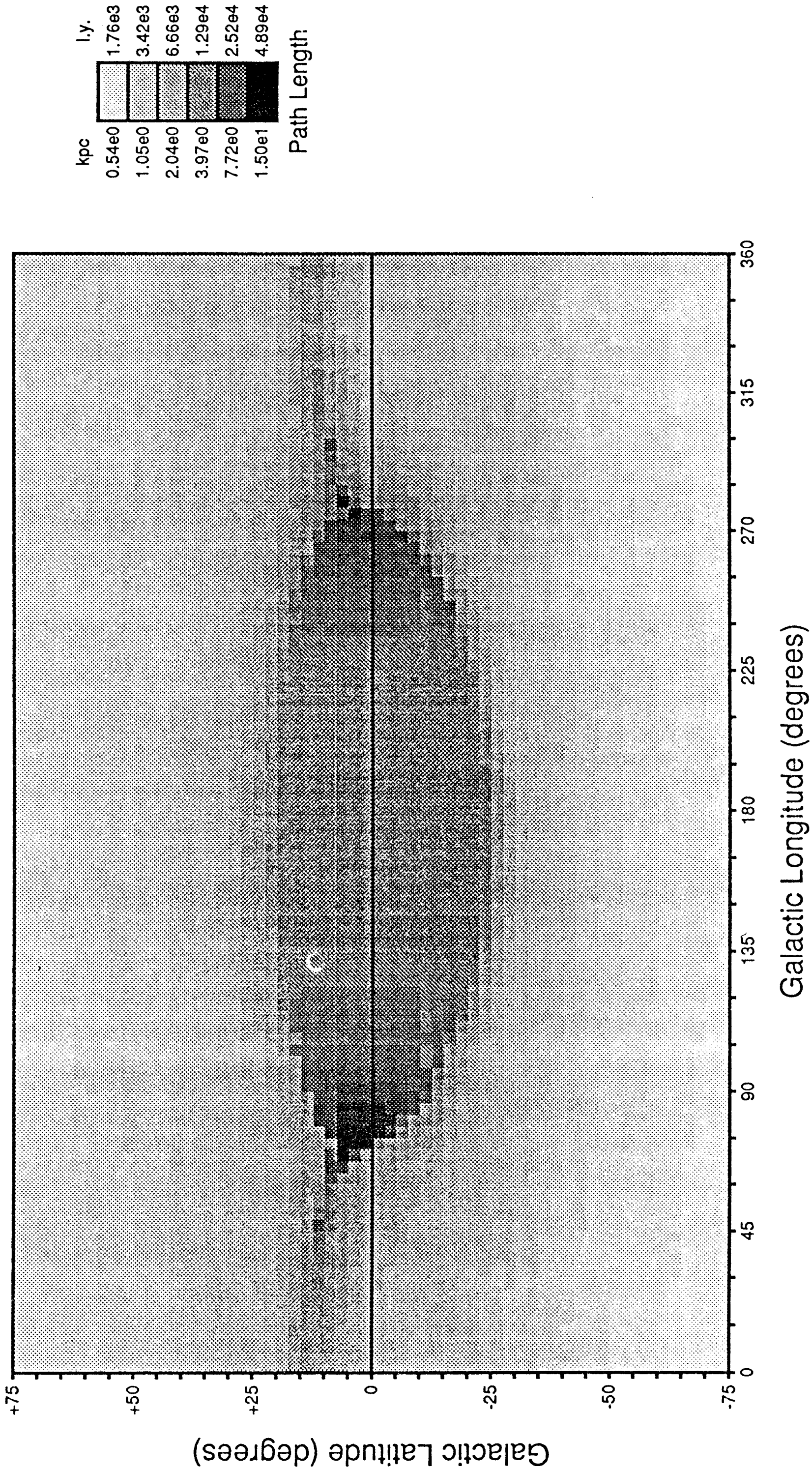
kpc
0.54e0
1.05e0
2.04e0
3.97e0
7.72e0
1.50e1
l.y.
1.76e3
3.42e3
6.66e3
1.29e4
2.52e4
4.89e4
Path Length
+75
+50
+25
0
-25
-50
-75
Galactic Latitude (degrees)
0
45
90
135
180
225
270
315
360
Galactic Longitude (degrees)

Fig. 2c

The data used for the generated maps were analysed to obtain first and second harmonics of the path length distribution in R.A. for comparison with observed anisotropies.

4. Results

Standard Galactic Field Model

Fig. 1 shows examples of path length distributions obtained for 10^{17}, 10^{18} and 10^{19} eV. Comparison may be made with Karakula *et al.* (1971) for the two higher energies and agreement is excellent both in the distribution in arrival directions and the magnitude of path lengths.

It is noteworthy that the path length distribution in celestial coordinates changes appreciably over this energy range. At 10^{19} eV (Fig. 1*c*) there is a clear galactic plane effect, whilst at 10^{17} eV (Fig. 1*a*) a quite different effect is clear. The change is clarified in Fig. 2 with results presented in galactic coordinates where it can be seen that to obtain the maximum galactic path length at 10^{17} eV it is necessary to launch antiprotons almost perpendicular to the local spiral arm field. Whilst progressively following the arm, they then spend the maximum possible time in the galaxy before reaching the extremities of the arm configuration. We note in Fig. 2*b* that for 50°N at 10^{18} eV a first harmonic (R.A.) amplitude of 54% is found (a latitude characteristic of the majority of observations at that energy). This amplitude is five times larger than experiment.

Modified Field Models

We recognise that our field model is oversimplified and we wished to investigate the effects of any modifications to the model. We first examined the effects of removing the field reversal at the galactic plane. This is part of the Thielheim–Langhoff model and has only limited supporting observational evidence. Fig. 3 shows as an example the path length distribution at 10^{18} eV for this model. The distribution has changed but the anisotropy is still great.

Berezinski and Mikhailov (1987) have discussed the possibility of a regular z (perpendicular to the galactic plane) component of the magnetic field disrupting propagation within the galaxy. We find, as they did, that a B_z can reduce the anisotropy (see Fig. 4 with a 34% anisotropy at 50°N), but we find that fields $B_z \approx 10^{-7} - 10^{-6}$ G are necessary to produce an appreciable change compared with values of $10^{-8} - 10^{-7}$ G found by Berezinski and Mikhailov (see Table 1).

It is possible that our galaxy has a halo which contains a significant magnetic field (Duric and Bloemen 1990). If this is so, it would be possible for a cosmic ray to leave the galactic plane and later return, possibly many times, after deflection within the halo. Such an effect would be likely to reduce the observable anisotropy as the trajectory is randomised. Fig. 5 shows the effect of a 1 μG halo field. Such a field is rather large (only slightly smaller than the disk fields). It reduces the northern anisotropy to about the level of the measured upper limit (9%) although, in this model, the southern anisotropy remains high at 34%. Rather similar magnitudes are found for a halo field either with lines parallel to the galactic plane or radial from the galactic centre.

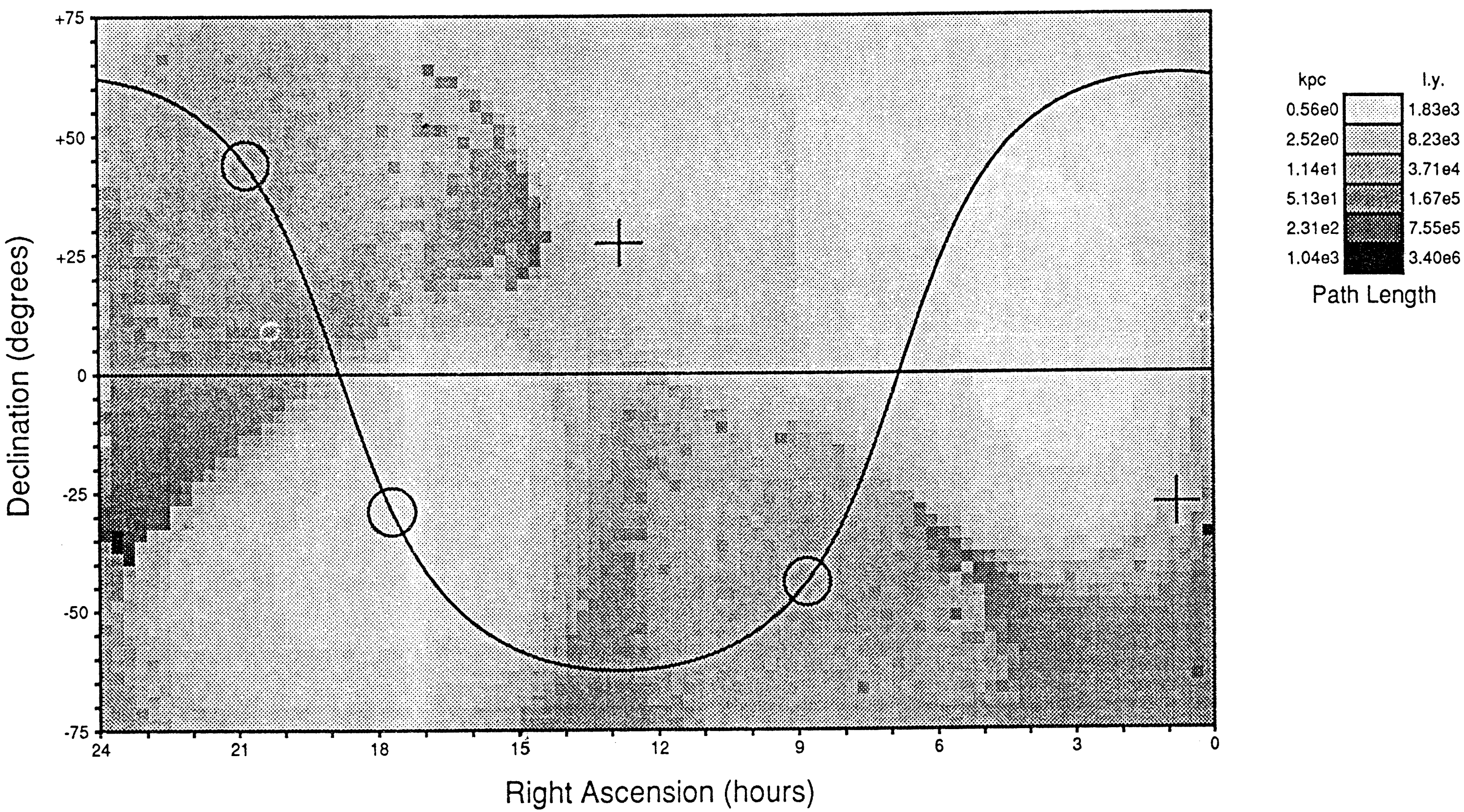

Fig. 3. Path length distribution for 10^{18} eV antiprotons in a Thielheim–Langhoff field model with field reversal at the galactic plane removed.

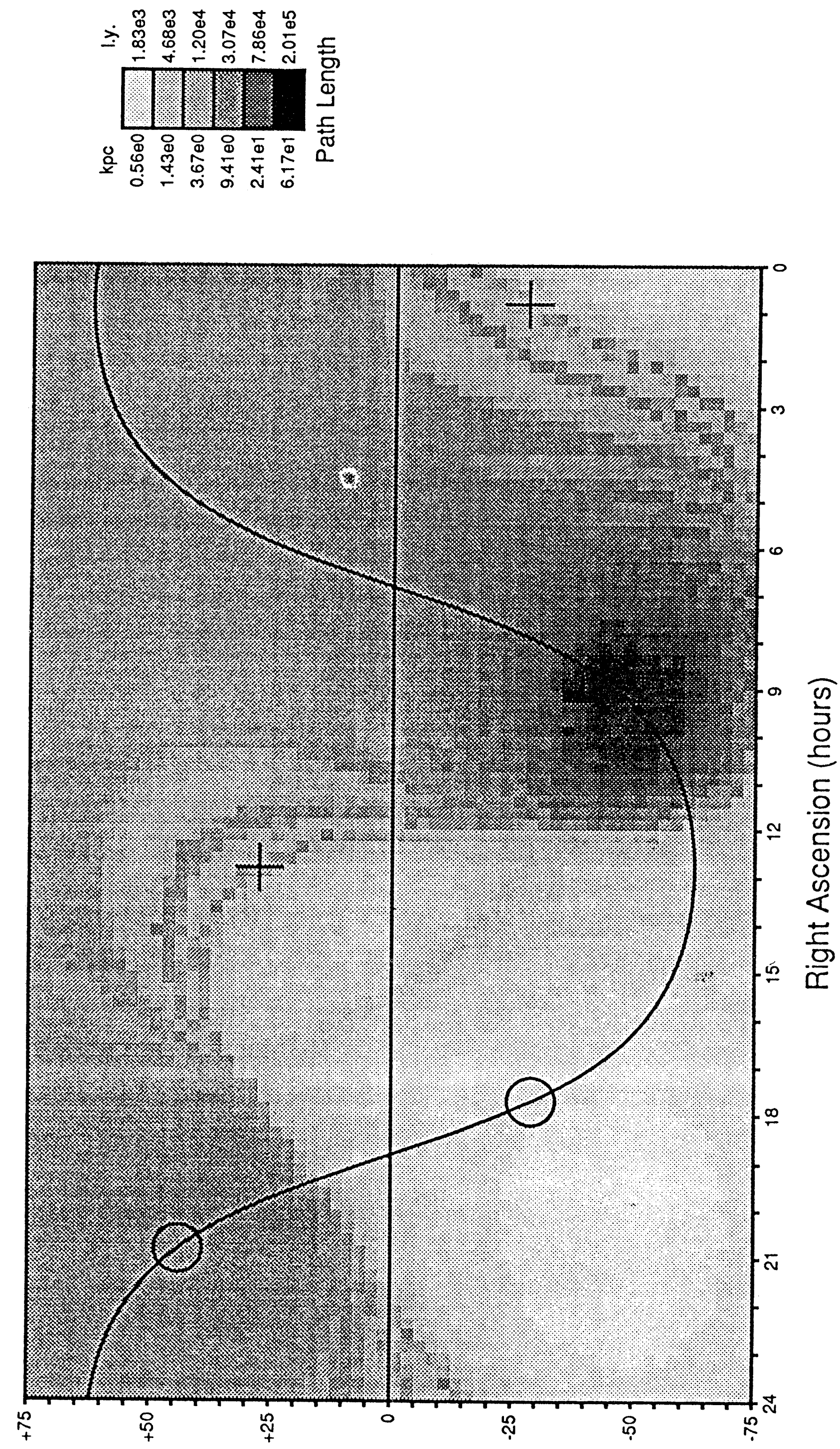

Fig. 4. Path length distribution for 10^{18} eV antiprotons in a Thielheim–Langhoff field model plus a constant magnetic field component of $0 \cdot 1$ μG perpendicular to the galactic plane.

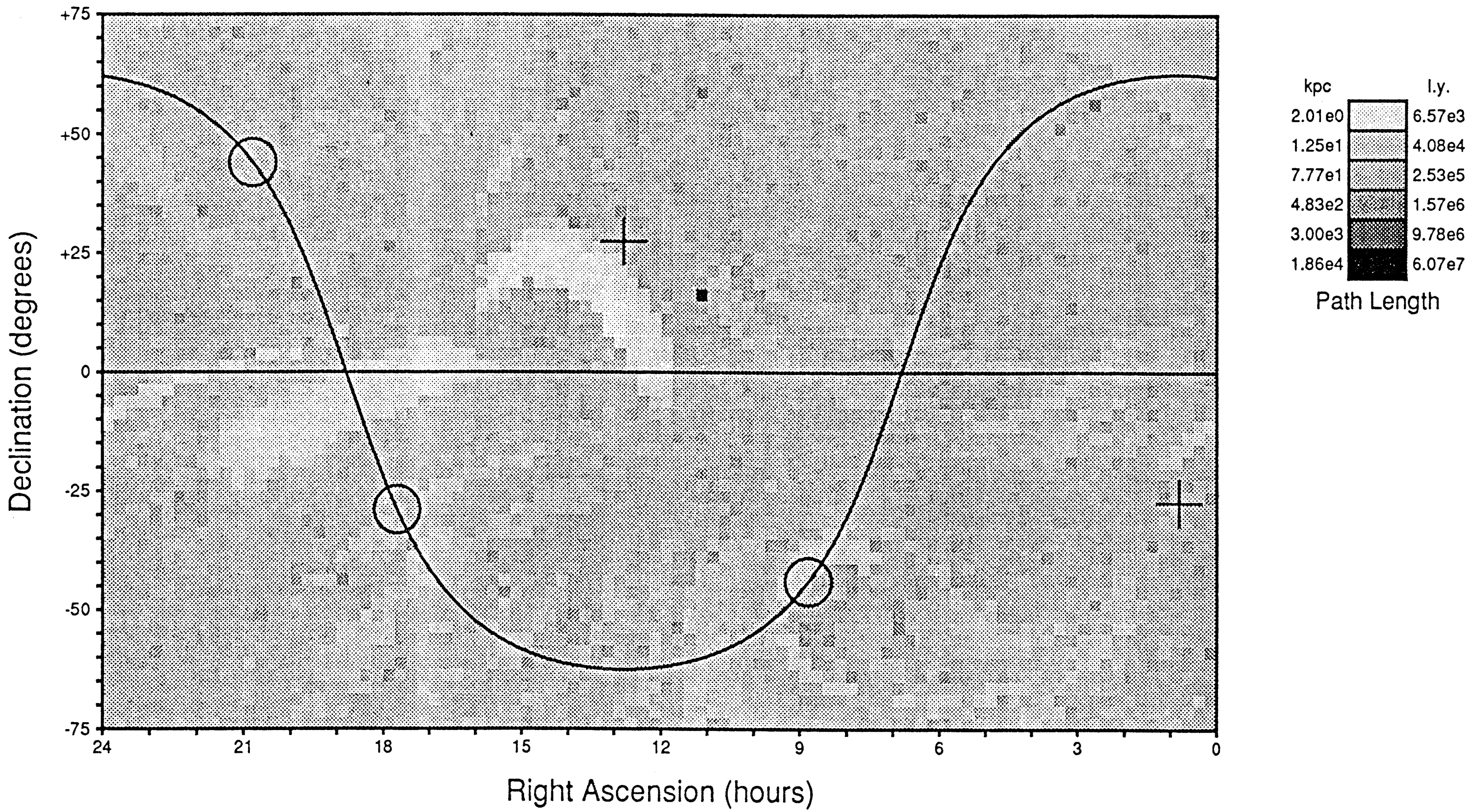

Fig. 5. Path length distribution for 10^{18} eV antiprotons in a Thielheim–Langhoff field model plus a halo field of 1 μG parallel to the galactic plane.

Table 1. Results for the standard Thielheim–Langhoff (1968) model with various values of B_z and energy 10^{18} eV

B_z (μG)	Mean lifetime (yr)	Northern hemisphere anisotropy Magnitude	Phase (hr)
0·000	$1 \cdot 5 \times 10^4$	0·54	21·1
0·010	$1 \cdot 5 \times 10^4$	0·50	21·3
0·032	$1 \cdot 5 \times 10^4$	0·46	21·3
0·1	$1 \cdot 7 \times 10^4$	0·34	21·6
0·316	$1 \cdot 4 \times 10^4$	0·15	2·8
1·000	$8 \cdot 4 \times 10^3$	0·22	22·0

Table 2*a*. Results for the standard Thielheim–Langhoff model

Energy (eV)	Mean lifetime (yr)	Northern hemisphere anisotropy Magnitude	Phase (hr)
$10^{18 \cdot 000}$	$1 \cdot 5 \times 10^4$	0·54	21·1
$10^{18 \cdot 250}$	$1 \cdot 1 \times 10^4$	0·66	23·4
$10^{18 \cdot 500}$	$8 \cdot 5 \times 10^3$	0·83	0·0
$10^{18 \cdot 750}$	$7 \cdot 3 \times 10^3$	0·86	0·4
$10^{19 \cdot 000}$	$6 \cdot 7 \times 10^3$	0·90	0·2
$10^{19 \cdot 250}$	$6 \cdot 3 \times 10^3$	0·87	0·1
$10^{19 \cdot 500}$	$6 \cdot 2 \times 10^3$	0·85	0·0
$10^{19 \cdot 750}$	$6 \cdot 1 \times 10^3$	0·81	0·1
$10^{20 \cdot 000}$	$6 \cdot 3 \times 10^3$	0·79	0·1
$10^{20 \cdot 50}$	$6 \cdot 4 \times 10^3$	0·79	0·1
∞	$6 \cdot 8 \times 10^3$	0·77	0·0

Table 2*b*. Standard Thielheim–Langhoff model with two scattering models at 10^{18} eV

The standard model refers to scattering due to random field directions, with model W retaining the field magnitude and model S having this increased by ten times in the scattering region

Scattering model	Mean lifetime (yr)	Northern hemisphere anisotropy Magnitude	Phase (hr)
None	$1 \cdot 5 \times 10^4$	0·54	21·1
W	$1 \cdot 2 \times 10^4$	0·36	23·8
S	$4 \cdot 2 \times 10^3$	0·26	5·1

It is likely that scattering of cosmic rays will occur in random components of the galactic field. However it should be noted that at 10^{18} eV a proton would have a gyroradius of 100 pc in a 10 μG field and thus any scattering structure would need to have very large dimensions in order to be effective. We have examined the effect of random variations in the direction and magnitude of the galactic magnetic field. In a model with randomised field directions, a random field direction was selected in one of each four (randomly chosen) 10 pc intervals along the trajectory (i.e. one per 40 pc). In order to also examine the effect of random magnetic field magnitudes, this scattering model was tested with the random field also being increased in magnitude by a factor of ten. These models were simple attempts to account for the measured random components of the galactic field (Rand and Kulkarni 1989) which have field strengths ranging from about 2 to 20 μG and scale lengths from 10 to 250 pc. At 10^{18} eV, the anisotropy reduced to ~26% for the strongest scattering effect.

5. Discussion

The results of our modelling are summarised in Table 2. It is clear that when a reasonable galactic magnetic field model is used and one considers the effect of a magnetic halo or significant scattering at 10^{18} eV, the magnitude of the predicted anisotropy for uniformly distributed galactic sources is always significantly above the generous 10% upper limit obtained from observation. It is possible that a combination of both these effects at the limit of their predictions might be compatible with observational upper limits at 10^{18} eV, but such a possibility may seem unlikely. Also, since experimental upper limits are set by the observing time and the array collecting area only, there is no particular reason to suspect that the underlying anisotropy is not well below the observed upper limits so that the galactic source model would fail completely.

It is also possible that the cosmic ray beam does not consist mainly of protons so that the appropriate rigidity to consider is related to momentum per charge. The 10^{19} eV upper limit is then much easier to accommodate in the model. However, the observational technique tends to favour the detection of protons in the beam (e.g. Clay 1985) and one would have to specify virtually no protons at a fixed energy in the beam, a supposition not favoured by experiment. One is thus drawn to the conclusion that at 10^{18} eV and above, the bulk of the cosmic ray beam has an extragalactic origin.

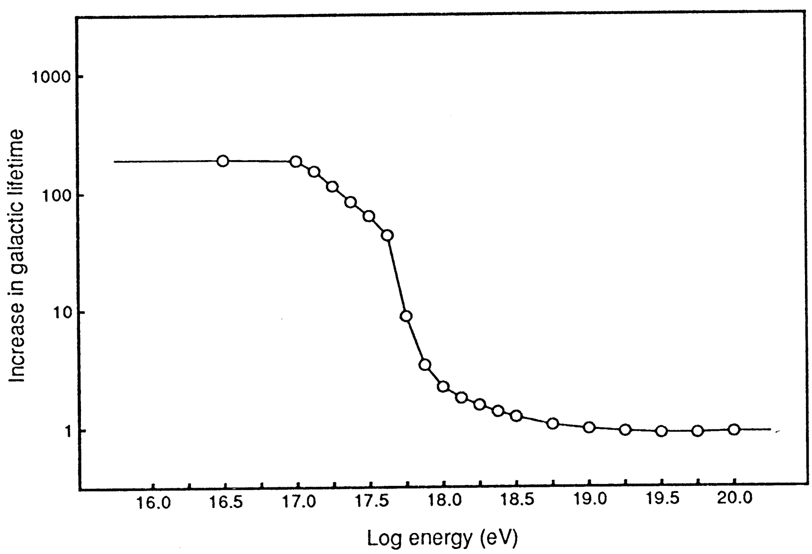

Fig. 6. Energy dependence of the average galactic lifetime of antiprotons fired from earth. A lifetime of $1 \cdot 0$ corresponds to about 10^4 yr.

At very low energies one presumes that most of the beam is of galactic origin since we know of some galactic sources with a total cosmic ray production rate sufficient to produce the observed flux. As an aside, Fig. 6 shows the variation of galactic lifetime with particle energy in our simple field model. The effect is that above 10^{18} eV there is little containment and, below $\sim 10^{17}$ eV, containment reaches a mean lifetime $\lesssim 2\times 10^{6}$ yr. This latter value, apparently continuing to low energies in this model, is approaching the observed low energy lifetime for cosmic rays (Webber 1990).

6. Conclusions

We have followed possible trajectories of cosmic ray particles in simple galactic magnetic fields and find that it is difficult, above an energy of $\sim 10^{18}$ eV, to reconcile observed anisotropies with a model assuming a uniform galactic source of cosmic rays. A dominating extragalactic source distributed broadly uniformly would be necessary, applying Liouville's theorem (Lemaitre and Vallarta 1933), to give the appropriate isotropy.

Acknowledgment

This work is supported by the Australian Research Council.

References

Berezinski, V. S., and Mikhailov, A. A. (1983). Proc. 18th Int. Cosmic Ray Conf., Bangalore, Vol. 2, p. 174 (Tata Institute of Fundamental Research: Bombay).

Berezinski, V. S., and Mikhailov, A. A. (1987). Proc. 20th Int. Cosmic Ray Conf., Moscow, Vol. 2, p. 54 (NAUKA: Moscow).

Cassiday, G. L., Cooper, R., Dawson, B. R., Elbert, J. W., Fick, B. E., Green, K. D., Ko, S., Liebing, D. F., Loh, E. C., Salamon, M. H., Smith, J. D., Sokolsky, P., Sommers, P., and Thomas, S. B. (1989). *Phys. Rev. Lett.* **62**, 383.

Clay, R. W. (1985). Proc. 19th Int. Cosmic Ray Conf., La Jolla., Vol. 9, p. 357 (NASA Conf. Publication 2376).

Clay, R. W. (1987). *Aust. J. Phys.* **40**, 423.

Duric, N., and Bloemen, H. (1990). Proc. 12th Int. Cosmic Ray Conf., Adelaide, Vol. 3, p. 217 (Univ. Adelaide).

Karakula, S., *et al.* (1971). Proc. 21st Int. Cosmic Ray Conf., Hobart, Vol. 1, p. 310 (Univ. Tasmania).

Lemaitre, G., and Vallarta, M. S. (1933). *Phys. Rev.* **43**, 87.

Linsley, J., and Watson, A. A. (1977). Proc. 15th Int. Cosmic Ray Conf., Plovdiv, Vol. 12, p. 203 (Bulgarian Acad. Sciences: Sofia).

Lyne, A. G., and Smith, F. G. (1989). *Mon. Not. R. Astron. Soc.* **237**, 533.

Murakami, K., Shibita, S., Fujii, Z., Yamada, T., Kojuma, H., Hayashida, N., and Kifune, T. (1990). Proc. 21st Int. Cosmic Ray Conf., Adelaide, Vol. 3, p. 192 (Univ. Adelaide).

Rand, R. J., and Kulkarni, S. R. (1989). *Astrophys. J.* **343**, 760.

Thielheim, K. O., and Langhoff, W. (1968). *J. Phys.* A **1**, 694.

Webber, W. R. (1990). Proc. 21st Int. Cosmic Ray Conf., Adelaide, Vol. 3, p. 393 (Univ. Adelaide).

Manuscript received 9 April, accepted 16 May 1990